J. Am. Ceram. Soc., 1–8 (2014)
DOI: 10.1111/jace.13125

journal

Toward Understanding the Effect of Low-Activity Waste Glass Composition on Sulfur Solubility

John D. Vienna,[‡,†] Dong-Sang Kim,[‡] Isabelle S. Muller,[§] Greg F. Piepel,[‡] and Albert A. Kruger[¶]

[‡]Pacific Northwest National Laboratory, Richland, Washington 99352

[§]Vitreous State Laboratory, The Catholic University of America, Washington, District of Columbia 20064

[¶]U.S. Department of Energy, Office of River Protection, Richland, Washington 99354

The concentration of sulfur in Hanford low-activity waste (LAW) glass melter feed will be maintained below the point where the salt accumulates on the melt surface. The allowable concentrations may range from near zero to over 2.05 wt% (of SO_3 on a calcined oxide basis) depending on the composition of the melter feed and processing conditions. If the amount of sulfur exceeds the melt tolerance level, a molten salt will accumulate which may upset melter operations and potentially shorten the useful life of the melter. At the Hanford site, relatively conservative limits have traditionally been placed on sulfur loading in melter feed, which in turn significantly increases the amount of LAW glass that will be produced. Crucible-scale sulfur solubility data and scaled melter sulfur tolerance data have been collected on simulated Hanford waste glasses over the last 15 years. These data were compiled and analyzed. An empirical model was developed to predict the solubility of SO_3 in glass based on 253 simulated Hanford LAW glass compositions. This model represents the data well, accounting for over 85% of the variation in data, and was well validated. The model was also found to accurately predict the maximum amount of sulfur in melter feed that did not form a salt layer in 13 scaled melter tests of simulated LAW glasses. The model can be used to help estimate glass volumes and make informed decisions on process options (e.g., scale of supplemental LAW treatment facility, and pretreatment facility performance requirements). The model also gives quantitative estimates of component concentration effects on sulfur solubility. The components that increase sulfur solubility most are $Li_2O > V_2O_5 > CaO \approx P_2O_5 > Na_2O \approx B_2O_3 > K_2O$. The components that decrease sulfur solubility most are $Cl > Cr_2O_3 > Al_2O_3 > ZrO_2 \approx SnO_2 >$ Others (i.e., the sum of minor components) $\approx SiO_2$. The order of component effects is similar to previous literature data, in most cases.

I. Introduction

The process deployed for nuclear waste glass vitrification in the United States includes feeding a slurry mixture of the nuclear waste and glass-forming additives on top of a molten glassmelt within ceramic lined melters. The melter feed slurry dries on the melt surface to form a cold-cap, which is heated by the glassmelt and reacts to form several intermediate products and ultimately forms the liquid silicate melt. Melter feeds with excess concentrations of certain anions will form a salt that accumulates on the melt surface. This salt contains primarily alkali- and alkaline-earth-sulfates, -phosphates, -chromates, -pertechnetates, -molybdates, and -halides. The salt creates several potential problems associated with melter operation including:[1–4] (1) it is corrosive to those melter components that contact it such as bubblers, thermowells, and even melt-line refractories; (2) it increases the volatility of technetium and cesium; (3) it increases the volatility of salts which can increase corrosion in the off-gas treatment system; (4) a glassmelt saturated in salt components may also form a water-soluble salt in the canistered glass which preferentially contains technetium, chromium, and cesium; (5) the molten salt may increase the risk of steam explosions; and (6) the salt layer may disrupt heating in the melt pool by forming low resistance current paths. Therefore, waste glass melters are generally operated in a way to avoid salt accumulation. Avoiding salt formation in the melter requires either (1) conservative empirical limits on salt-forming components such as sulfur, chromium, and halides or (2) a model able to predict the practical limit of salt solubility in the melter as a function of melter feed composition. In addition to avoiding salt accumulation in the melter, methods for detecting the presence of salt and destroying accumulated salts have been developed. For the purposes of this article, the term sulfur tolerance is defined as the maximum amount of sulfur in melter feed that did not form a measureable salt layer in the melter operated at the nominal conditions and rates of the Hanford LAW melter.

Sulfur can be incorporated into silicate glass melts in a range of oxidation states from sulfate (SO_4^{2-}) to sulfide (S^{2-}).[5–8] In U.S. nuclear waste glass melts, sulfur occurs primarily in the form of a sulfate ion.[9–13] However, under extreme reducing conditions, sulfide may be generated in waste glass melts and form metal sulfide liquids that reduce melter life.[9,14] In the silicate melt, sulfate ions form primarily isolated tetrahedra associated with either alkali or alkaline-earth ions.[10,15–19] The molten salt identified in U.S. LAW and high-level waste (HLW) glass melters primarily contained sulfur in the sulfate state. This salt is primarily sodium sulfate with smaller amounts of other alkali, alkaline earths, chromate, phosphate, chloride, molybdate, pertechnetate, fluoride, and other oxyanionic salts.[4,20–26]

There are kinetic aspects to sulfate incorporation into the melt. Generally, an oxyanionic salt is formed in the cold-cap that is dominated by volatile salts such as nitrates, nitrites, and hydroxides (sometimes called primary melt).[27,28] As the temperature of the salt increases, the major components (nitrates, nitrites, hydroxides, etc.) of the primary melt decompose and/or volatilize leaving the less volatile salt components (sulfates, phosphates, etc.).[29] The resulting salt is partially incorporated into the silicate melt, is partially volatilized, and may partially accumulate as a salt segregated from the cold-cap. The fraction of sulfur that volatilizes is highly dependent on both the contents of sulfur and reducing agents in the batch.[3,22,30–32] Additionally, sulfate dissolved in

C. Jantzen—contributing editor

Manuscript No. 34338. Received January 6, 2014; approved June 10, 2014.
[†]Author to whom correspondence should be addressed. e-mail: john.vienna@pnnl.gov

the silicate melt may separate from the melt under conditions that change its solubility. The result of these kinetic processes is that salt segregation/accumulation may occur at sulfur concentrations well below the thermodynamic solubility of sulfate in the melt composition and temperature.[3,20,29] The solubility of sulfate in silicate melts can be readily measured in the laboratory with standard equipment and approaches. However, it is not currently clear how thermodynamic solubility of sulfate correlates to the concentration of sulfate in the melter feed that will accumulate as a salt during normal melter processing. Such accumulation may be determined by kinetic factors. Yet, it can be theorized that the higher the thermodynamic solubility, the higher the amount of sulfate that can be fed to the melter without accumulating a salt phase.[31,33] This challenge is addressed later in the article.

Several attempts have been made to correlate the propensity for salt accumulation as a function of melter feed composition. These attempts invariably start with a solubility limit or tolerance for sulfate ion (SO_4^{2-}) or sulfur trioxide (SO_3) as a function of melt or melter feed composition. Papadopoulos developed a model of SO_3 solubility in soda-lime-silicate melts based on the estimated concentration of nonbridging oxygen (NBO) per tetrahedron.[34] Li *et al.* adopted the Papadopoulos approach to Hanford LAW and HLW glasses.[35] Ooura and Hanada found that for (1) binary alkali-silicate glasses, the ratio of NBO to bridging oxygen predicted well the sulfate solubility, and (2) ternary alkaline earth-alkali-silicate glasses, the impact of alkaline-earth oxide concentration on sulfate solubility was linear and the slope was dependent on the thermal decomposition equilibrium constant of the metal sulfate.[36] Pelton applied a CALPHAD methodology (using a modified Reddy-Blander model) to fit composition effects on sulfate solubility in five component (SiO_2, Al_2O_3, CaO, MgO, and Na_2O) silicate melts.[37] Pegg *et al.* suggested a solubility product-type relationship between Na_2O and SO_3 in Hanford LAW glass melts as a practical minimum waste loading target for the WTP LAW vitrification system such that:

$$g_{Na_2O} \times g_{SO_3} \leq 0.0005$$

where g_i is the ith component mass fraction in glass.[3] Schreiber and Stokes propose that glass basicity and oxygen potential will dictate sulfate solubility in Hanford HLW melts.[38] Peeler *et al.* developed a conservative single-value limit of 0.6 wt% (as SO_4^{-2}) in Savannah River HLW melts for application to the Defense Waste Processing Facility (DWPF),[21,39] which may be increased slightly by adding V_2O_5.[40] Vienna *et al.* determined a similar single-value limit for Hanford LAW glass of 0.8 wt% SO_3.[33] Jantzen *et al.* correlated the salt formation limit in sealed crucible tests of simulated DWPF HLW glasses to viscosity of the melt which in turn was correlated with NBO concentrations.[2] Manara *et al.* correlated the sulfate solubility in simplified commercial HLW glass melts to the ratio of alkali to boron concentrations and attributed the impact of V_2O_5 to increasing sulfate solubility and increasing the kinetics of sulfur incorporation through depolymerization of the borosilicate network.[41] Bingham correlated the effects of component concentrations on the SO_3 solubility and incorporation in multicomponent phosphate glasses to the field strength of the components and proposed that the same correlation would be valid for silicate-based waste glass melts.[42,43] Billings and Fox found that increasing CaO and B_2O_3 in frit and lowering alkali increase the sulfur retention in sealed crucible tests with simulated Savannah River HLW glass melts.[44]

Overall, the literature contains some conflicting results, but it is clear that SO_3 solubility is highly compositionally dependent. Nuclear waste vitrification at the Hanford site requires near real-time glass formulation to meet project goals and complete the tank waste cleanup mission in an effective manner. To implement such a strategy, a quantitative model is needed to predict SO_3 tolerance based on melter feed composition. None of the approaches discussed above have been found appropriate for implementation at Hanford. This article documents the initial attempt to develop a model to predict SO_3 tolerance in Hanford LAW glasses based on melter feed composition.

II. Experimental Data

Several series of experiments were performed to measure the solubility of SO_3 in simulated Hanford LAW glasses at crucible scale and to measure the tolerance for SO_3 in the feed by scaled melter tests. These data and the associated experimental methods are summarized here and are also documented in more detail in recently released U.S. Department of Energy project reports by the Catholic University of America (see references inscribed in Table I). These data are summarized below.

(1) Saturation Method

The solubility of SO_3 in simulated waste glass melts was measured by supersaturating the melt with Na_2SO_4 in the amount of several wt% (typically 4 wt%) of SO_3 in the glass if 100% was retained. The mixtures of glass powder and Na_2SO_4 were melted at 1150°C in Pt alloy crucibles (without forced mixing) with a cover in resistance-heated furnaces. After a melting period of roughly 1 h, the melt blanketed by a molten salt layer was cooled naturally to room temperature in an air atmosphere furnace. Then the glass, covered with a sulfate salt layer, was recovered for examination. After washing the broken glass chunks to remove the segregated salt, the glass was ground and washed in dilute nitric acid to remove remaining salt inclusions. The composition of the glass was then analyzed using X-ray fluorescence (XRF) to determine the resulting SO_3 concentration in glass. The SO_3 concentrations measured by this method are labeled $w_{SO_3}^{Sat}$. Using Na_2SO_4 to supersaturate the melt minimizes any sodium deviation in the final glass phase by the exsolution of an uncontrolled amount of the Na_2SO_4 phase.

(2) Bubbling Method

The solubility of SO_3 in simulated waste glass melts was measured using a gas bubbling system. The glasses were melted at 1150°C in a Pt alloy crucible under flowing mixtures of SO_2, O_2, and N_2 to achieve the desired partial pressure of SO_3 (p_{SO_3}). Samples of the glassmelt were taken and analyzed for SO_3 concentration by XRF as a function of p_{SO_3}. The experiments were continued until the melt was saturated with SO_3 (that is, the concentration of SO_3 in the glass no longer changed with p_{SO_3}). Saturation of the melt often occurred later than the formation of a segregated salt layer on the surface of the melt, so, the glass was ground

Table I. Summary of SO_3 Solubility and Melter Tolerance Data for Hanford Simulated LAW Glasses

Source	Saturation	Bubbling	Melter	Total
Muller *et al.*[45]	0	1†	0	1
Muller *et al.*[46]	42	0	0	42
Muller and Pegg[47]	55	1†	0	55
Matlack *et al.*[48]	14	1	1	14
Matlack *et al.*[49]	4	4	1	4
Matlack *et al.*[50]	36	15	2	36
Matlack *et al.*[51]	41	13	4	41
Matlack *et al.*[52]	41	2	3	41
Muller *et al.*[53]	30	1	2	30
Total	263	38	13	264

†Glass compositions are reported in the document listed in the source column, while $w_{SO_3}^{Bubb}$ values are reported by Matlack *et al.*[48]

and washed with dilute nitric acid prior to XRF to remove any salt inclusions. The SO_3 solubilities measured by this method are labeled $w_{SO_3}^{Bubb}$.

(3) Scaled Melter Tests

Melter tests were performed in the Duramelter (DM)-10, -100, and -1200 melter systems located at the Vitreous State Laboratory of The Catholic University of America. These melter systems are scaled, prototypical Hanford melters with Inconel Joule-heating electrodes, high-chromium refractory liners, and air bubblers. The simulated nuclear waste was blended with prototypic Hanford glass-forming chemicals in ratios to obtain the target glass composition. The resulting slurry feed was fed onto the top of the bubbled melt pool where it reacted to form the molten silicate melt and, in the case of excessive SO_3, a molten salt. The nominal melt pool operating temperature was maintained at roughly 1150°C and the plenum temperature ranged between roughly 500°C and 700°C. The melters were bubbled with air at a rate adjusted to maintain a nominal glass processing rate of roughly 2000 $kg_{glass}/m^2/d$. Sugar was added to the melts to facilitate the decomposition of nitrate and nitrite components of the waste simulant using a fixed ratio of 0.75 mol of organic carbon to each mole of NO_x in the melter feed. This reductant ratio and the air bubbling maintained the iron oxidation state of the glassmelt well below 10% Fe(II)/Fe (Total), ensuring sulfur was incorporated as sulfate. The presence or absence of an accumulated salt was determined by (1) reaching steady-state melting conditions with the feed, (2) stop feeding and allowing the cold-cap to completely react into the melt, and (3) probing the surface with a rod to determine if salt was present. When probing the surface, the salt readily wets the all-thread rod making it easy to detect even small pockets of salt on the surface of the small melters. For the larger melters, multiple melt surface locations must be probed to determine if any salt is present. The concentration of SO_3 was then changed to narrow the maximum concentration that did not form a salt and the minimum concentration of SO_3 that did form a persistent salt. The SO_3 tolerances measured by this method are labeled $w_{SO_3}^{Melt}$.

(4) Data Summary

The resulting data are summarized in Table I. The composition region covered by these 264 glasses is summarized in Table II. There is generally good concentration distribution for each of these components, with a few exceptions:

1. One glass (LAWA55) contained 7.9 wt% BaO, the concentration in all other glasses was ≤0.01 wt%.
2. One glass (LAWA58) contained 5 wt% Bi_2O_3, no other glass contained any.
3. One glass (LAWA62) contained 3 wt% CoO, no other glass contained any.
4. One glass (LAWA63) contained 3 wt% CuO, no other glass contained any.
5. One glass (LAWABPS) contained 2 wt% each of Gd_2O_3 and La_2O_3, only one other glass contained any Gd_2O_3 and one other glass contained any La_2O_3.
6. One glass (LAWA92) contained 7.9 wt% Gd_2O_3.
7. One glass (LAWA91) contained 7.9 wt% La_2O_3.
8. One glass (LAWA61) contained 2.5 wt% MnO, the concentration in all other glasses was ≤0.06 wt%.
9. One glass (LAWA59) contained 3 wt% Sb_2O_3, no other glass contained any.
10. Two glasses (LAWA54 and LAWA72) contained 7.9 wt% SrO, the concentration in all other glasses was ≤ 0.08 wt%.

These 11 glasses with extreme component concentrations were excluded from the modeling dataset, leaving 253 glasses. The resulting component concentration ranges are also summarized in Table II along with the centroid composition which is the mean composition of the 253 glasses in the modeling dataset.

Table II. Component Concentration (Normalized wt% Without SO_3) Ranges in Simulated LAW Glasses

	Full Dataset (264)		Model Dataset (253)		
Component	Min	Max	Min	Max	Centroid
Al_2O_3	5.53	13.95	5.53	13.95	8.22
B_2O_3	3.98	16.06	3.98	16.06	9.84
BaO	0	7.90	0	0.01	0.00
Bi_2O_3	0	5.01	0	0	0
CaO	0	12.94	0	12.94	6.17
CdO	0	0.24	0	0.24	0.00
Cl	0	1.17	0	1.17	0.40
CoO	0	3.05	0	0	0
Cr_2O_3	0.01	1.00	0.01	1.00	0.26
Cs_2O	0	0.19	0	0.19	0.03
CuO	0	3.05	0	0	0
F	0	3.06	0	3.06	0.09
Fe_2O_3	0	13.54	0	13.54	2.04
Gd_2O_3	0	7.90	0	0	0
K_2O	0.11	8.34	0.11	8.34	1.18
La_2O_3	0	7.90	0	0	0
Li_2O	0	5.86	0	5.86	1.17
MgO	0	10.10	0	10.10	1.61
MnO	0	2.50	0	0.06	0.00
MoO_3	0	0.01	0	0.01	0.00
Na_2O	2.48	26.05	2.48	26.05	17.93
NiO	0	0.11	0	0.11	0.00
P_2O_5	0	3.08	0	3.08	0.15
PbO	0	0.07	0	0.07	0.00
Re_2O_7	0	0.10	0	0.10	0.02
Sb_2O_3	0	3.00	0	0	0
SiO_2	30.05	50.64	30.05	50.64	41.69
SnO_2	0	5.01	0	5.01	0.78
SrO	0	7.90	0	0.08	0.00
TiO_2	0	4.11	0	4.11	0.40
V_2O_5	0	4.39	0	4.39	0.69
ZnO	0	5.86	0	5.86	3.17
ZrO_2	2.62	9.02	2.62	9.02	4.14

Figure 1 shows the pairwise comparisons of major component concentrations for the 253 glass compositions in the dataset as a scatterplot matrix. The data do not provide full coverage of the space for some pairs of components because as glass formulations evolved, some components were added to replace other components. As examples, older glasses (prior to 2005) contain significant Fe_2O_3 and TiO_2 while newer LAW glasses don't, and newer glasses contain significant concentrations of SnO_2 and V_2O_5 while older glasses don't.

Sufficient glass compositions had their SO_3 solubilities/tolerances measured by the three different methods to permit comparing the results. Figure 2 compares the melter tolerance for SO_3 ($w_{SO_3}^{Melt}$, the value that truly needs to be controlled during glass production) with the results from the two crucible melt techniques ($w_{SO_3}^{Bubb}$ and $w_{SO_3}^{Sat}$). The $w_{SO_3}^{Bubb}$ correlated strongly with $w_{SO_3}^{Melt}$. Correlating $w_{SO_3}^{Bubb}$ to $w_{SO_3}^{Melt}$ resulted in a line with the intercept and slope not being statistically different from 0.0 and 1.0, respectively, an $R^2 = 0.92$, and a root mean squared error (RMSE) = 0.094 wt%. Likewise, correlating $w_{SO_3}^{Sat}$ to $w_{SO_3}^{Melt}$ resulted in a line with $R^2 = 0.82$ and RMSE = 0.13 wt%. The slope was not statistically different from 1.0, but there was a statistically significant offset (or intercept) of $w_{SO_3}^{Melt} - w_{SO_3}^{Sat} = 0.2115$ wt%. These strong correlations between results from crucible scale testing and melter testing suggest that, under the conditions used for these tests and the composition region investigated, solubility

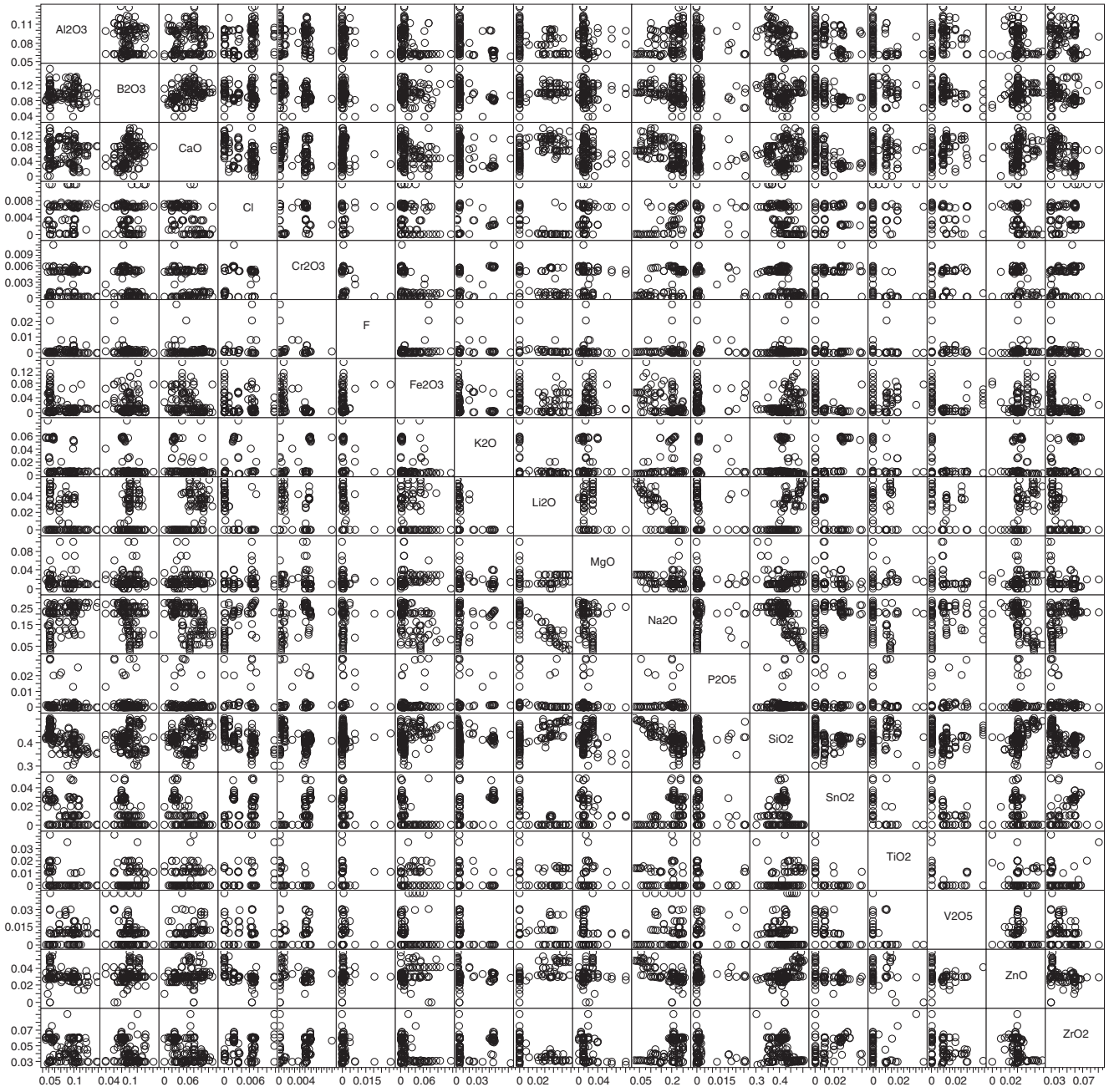

Fig. 1. Scatterplot matrix of component concentrations (normalized mass fractions) in the modeling dataset.

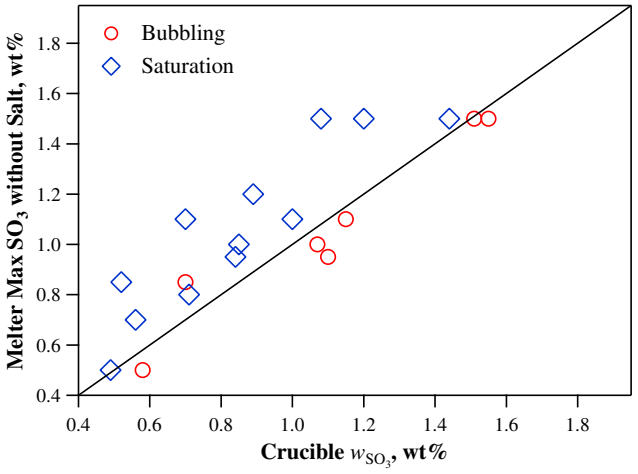

Fig. 2. Comparison of $w_{SO_3}^{Melt}$ to $w_{SO_3}^{Bubb}$ (circles) and $w_{SO_3}^{Sat}$ (diamonds).

data from crucible testing can be used to predict SO_3 tolerance in the melter feed. Hence, the much more abundant crucible scale data can be used to predict the effect of glass composition on SO_3 tolerance in the melter.

III. Model Development

To correlate melt composition to the SO_3 tolerance, the data were modified to form a modeling dataset. Because of the scarcity of $w_{SO_3}^{Melt}$ data (13 compositions), it was decided to perform the modeling on crucible scale data only and reserve melter scale data for validation. Because bubbling solubility data matched melter tolerance more closely, the modeling dataset used $w_{SO_3}^{Bubb}$ for any glass with bubbling data available (38 data points) and $w_{SO_3}^{Sat}$ + offset (=0.2115) for all other glasses (215 data points). The symbol w_{SO_3} is used to represent both the $w_{SO_3}^{Bubb}$ and $w_{SO_3}^{Sat}$ + offset data. Each target glass composition was normalized after removing SO_3 from the composition for three reasons: (1) the SO_3 obtained in the

glass was substantially different from the target, (2) the basis for target SO_3 was different for the two methods used, and (3) w_{SO_3} was the independent variable being modeled. The following equation was used to normalize the compositions.

$$n_i = \frac{g_i}{1 - g_{SO_3}},$$

where g_i is the ith component mass fraction in glass and n_i is the normalized mass fraction of the ith component so that the normalized concentrations of all components ($i = 1, 2, \ldots, q$) except SO_3 sum to 1.

The resulting dataset of 253 glass compositions was used to develop quantitative models between n_i and w_{SO_3}. A partial quadratic mixture model[54] was found to be the most successful at both fitting the w_{SO_3}data and being validated by data not used to fit the model. This model has the general form

$$w_{SO_3}^{Pred} = \sum_{i=1}^{q} s_i n_i + \text{selected}\left\{ \sum_{i=1}^{q} s_{ii} n_i^2 + \sum_{j=1}^{q-1} \sum_{k=j+1}^{q} s_{jk} n_j n_k \right\}$$

where $w_{SO_3}^{Pred}$ = predicted SO_3 solubility (in wt%), q = number of components in the waste glass, except for SO_3, n_i = normalized (after removing SO_3) mass fraction of the ith component, s_i = coefficient of the ith component, s_{ii} = coefficient for the ith component squared, s_{jk} = coefficient for the jth and kth components crossproduct.

The data for the 253 simulated LAW glasses were initially fit to the first-order form of the model (i.e., s_{ii} and s_{jk} values equal to zero) to determine which components had a significant impact on w_{SO_3}. JMP® 10.0.2 software (SAS Institute Inc., Cary, NC) was used to fit the first-order model initially using all components with a maximum concentration (in at least one glass) of 0.2 wt% or greater. The component effects (slope of $w_{SO_3}^{Pred}$ versus n_i) and their uncertainties were calculated based on the data centroid composition (given in Table II) using Eqs. (12) to (16) of Piepel.[55] The components with the least significant slopes were removed from the fit and included into a grouped "Others" component along with the components with concentrations less than 0.2 wt%. Slope significance was judged at the 90% confidence level. The component with the least significant overlap was removed first and the model refit. This process was repeated until R_p^2 statistics began to increase. The R_p^2 statistic represents the fraction of variability in the w_{SO_3} data values accounted for by the fitted model, where each data point is "left out of the fit" in evaluating how well the model predicts that data point. R_p^2 estimates the fraction of variability that would be accounted for in predicting new observations drawn from the same composition space. The order of components moved to Others was (from least to highest significance): Fe_2O_3, ZnO, MgO, TiO_2, and F. This left a first-order model containing: Li_2O, CaO, V_2O_5, Na_2O, B_2O_3, Al_2O_3, Cl, Cr_2O_3, ZrO_2, K_2O, P_2O_5, SnO_2, SiO_2 and Others (in order of significance). The slopes for SiO_2 and SnO_2 were nonsignificant at the 90% level. However, it was decided to retain separate model terms for SiO_2 and SnO_2.

The squared terms (n_i^2) and crossproduct terms ($n_j n_k$) used in the model fit were selected to give the best combination of model fit and model validation statistics while minimizing the number of second-order terms. Four candidate models were selected based primarily on their R_p^2 statistics and general knowledge of component effects on w_{SO_3}: (1) a model with 14 first-order terms, (2) a model with 14 first-order terms plus a $Li_2O \times Li_2O$ term, (3) a model with 14 first-order terms plus $Li_2O \times Li_2O$ and $CaO \times Cr_2O_3$ terms, and (4) a model with 12 first-order terms (without K_2O and SnO_2 terms) plus a $Li_2O \times Li_2O$ term. The fourth model excluded K_2O and SnO_2 because they were the least significant terms when the $Li_2O \times Li_2O$ term was added. Each of the four candidate models was fitted and then validated (as described below). The model with the best validation performance was then selected as the final model. Four data points were consistently found to be outliers (with residuals greater than three standard deviations)—LAWA76, LAWB102, LAWB104, and LAWB67S4. When they were removed from the various fits, the fit statistics were improved but the model coefficients remained almost unchanged. An examination of their compositions and w_{SO_3} values didn't show any trends. It was therefore decided to leave the outliers in the modeling dataset.

Models were also fitted to composition data converted into mole fractions of components. The significant terms and model statistics were found to be roughly the same. Slightly higher R_p^2 statistics were obtained from the mass-fraction models, so those models are reported in this article.

Table III lists the final model components and coefficients, where it is seen that 15 terms appear in the model (the components not listed as specific terms are included in the Others component) and that only one quadratic term ($Li_2O \times Li_2O$) appears. Table IV lists the summary statistics for the model fit, where it is seen that the values for R^2, R_A^2, and R_p^2 are very close, suggesting that there are no unnecessary model terms and no significantly outlying or influential data points.

Figure 3 shows a plot of the predicted ($w_{SO_3}^{Pred}$)and measured (w_{SO_3}) experimental data with 90% prediction intervals. Prediction intervals that overlap the 45° line indicate that the model predicts w_{SO_3} within the uncertainty of the model. The corresponding 90% prediction intervals generally overlap the 45° line, although the model tends to slightly underpredict w_{SO_3} values above roughly 1.4 wt%. A slight underprediction is not a concern for the intended use of the model as it will result in conservative formulations.

Table III. List of Model Components and Coefficients

Model Term	Coefficient
Al_2O_3	−2.091901
B_2O_3	3.0440748
CaO	4.4422886
Cl	−22.65353
Cr_2O_3	−13.14139
K_2O	0.615785
Li_2O	2.4739255
Na_2O	2.8972089
P_2O_5	4.606083
SiO_2	0.2407285
SnO_2	−1.775325
V_2O_5	7.5345478
ZrO_2	−1.871916
Others†	−0.280272
$Li_2O \times Li_2O$	260.20302

†Others is the sum of all components not specifically listed as model terms (i.e. those not anticipated to have a significant effect).

Table IV. Model Fit Summary Statistics

Summary Statistics	Value
N	253
p	15
Mean	1.004
R^2	0.8910
R_A^2	0.8846
R_P^2	0.8735

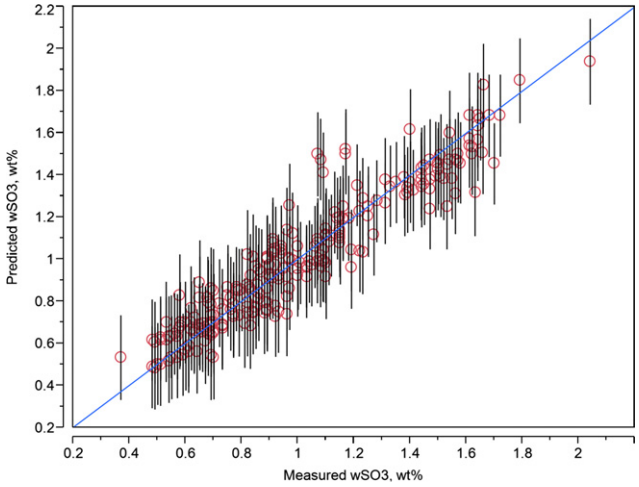

Fig. 3. Comparison of predicted and measured $w_{SO_3}^{Pred}$ with 90% prediction intervals (wt%).

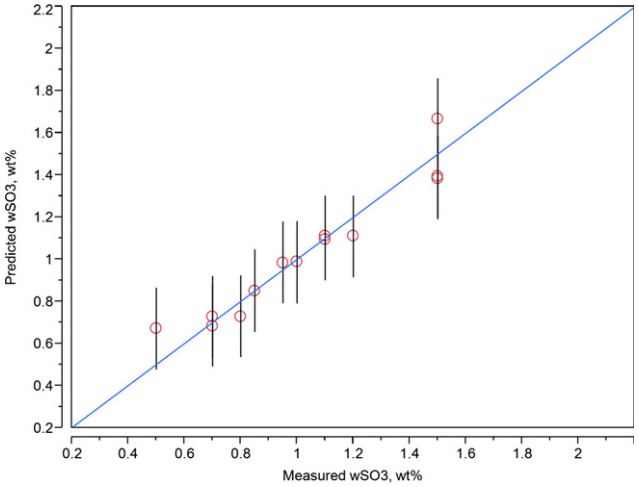

Fig. 4. Comparison of predicted $w_{SO_3}^{Pred}$ (based only on crucible scale data) with the measured maximum concentration of SO_3 in a melter test without salt accumulation ($w_{SO_3}^{Melt}$).

Two approaches were used to validate the model in Table III, namely (1) subsetting the dataset used to fit the model (i.e., cross-validation), and (2) validating with data not used in model fitting. To subset the data, they were first sorted by $w_{SO_3}^{Pred}$ values. The data were then numbered 1, 2, 3, 4, 5, 1, 2, … to split them into five representative groups each containing roughly 20% of the data. The same model form (including the same set of terms) was fit to each group of four of the five subsets of data and used to predict SO_3 solubility in the remaining validation subset. Table V summarizes the results of this model validation exercise. The R^2 value for the fit of each subset model are all close to each other at approximately 0.89. The validation R^2 (R_V^2) values range from 0.84 to 0.91, which are sufficiently close to the model fit R^2 values in Table V and the R^2 value in Table IV. The average R_V^2 value of 0.87 in Table V is also very close to the R_p^2 value of 0.87 in Table IV. Based on the results of this validation approach, it is reasonable to expect that 87% of the variation in newly generated data within the same composition space will be accounted for by this model. The variation not accounted for by the model can be addressed using statistical methods for calculating the uncertainty in model predictions.

For the second validation approach, the model was used to predict the maximum concentration of SO_3 from scaled melter tests that did not accumulate a salt layer ($w_{SO_3}^{Melt}$). These data were not used to fit the model and hence serve to validate it. More importantly, $w_{SO_3}^{Melt}$ is the property that must be predicted to successfully operate the Hanford LAW glass melters. Figure 4 compares the model-predicted $w_{SO_3}^{Pred}$ values with the measured $w_{SO_3}^{Melt}$ values for the 13 glasses having such data. A good correlation is obvious from the figure with an R_{V^2} for this dataset of 0.93. The root mean squared prediction error (RMSPE) = 0.086 is slightly smaller than the RMSE = 0.12 from the model fit.

Two conclusions can be drawn from the results of the two validation approaches. First, the model predicts w_{SO_3} for data not used to fit the model as well as it predicts data used to fit the model. Second, a model based on crucible-scale solubility data ($w_{SO_3}^{Sat} \pm$ offset and $w_{SO_3}^{Bubb}$) can be used to predict the maximum allowable SO_3 in the melter feed ($w_{SO_3}^{Melt}$). This directly addresses the "challenge" of how to relate sulfur solubility measurements with salt formation in the dynamic melter process. In the case of the limited system reported here there is a direct correlation between $w_{SO_3}^{Melt}$ and $w_{SO_3}^{Pred}$ (based on crucible-scale solubility data).

Also, $w_{SO_3}^{Pred}$ values were calculated for the 11 glasses removed from the model dataset as composition outliers. The w_{SO_3} values for all 11 data points were underpredicted, while the 90% prediction intervals overlapped the w_{SO_3} values for 9 of the 11 points. The remaining two glasses were significantly underpredicted—LAWA55 with 8 wt% BaO and LAWA54 with 7.9 wt% SrO. This trend matches previous expectations that the alkaline-earth components should increase w_{SO_3}, which is not well predicted by the Others term (that slightly decreases $w_{SO_3}^{Pred}$).

IV. Discussion

A model of SO_3 solubility in waste glasses was empirically fit to simulated Hanford LAW glass composition data. Not only were the model coefficients empirically fit, but also to some extent the model form was selected empirically. Figure 5 is a response-trace plot (sometimes referred to as a "spider-plot")[56] that shows the effects of individual component concentration changes on $w_{SO_3}^{Pred}$. Each curve on the figure spans the range of the corresponding component concentration in the database and is centered on the average composition of the test data used to fit the model (i.e. the centroid). The centroid composition and calculated component effects (slopes) at that centroid are listed in Table VI. The slopes for all components in the model (except n_{Li_2O}) are nearly constant, while the slope for n_{Li_2O} depends on its concentration. The slope for n_{Li_2O} at the centroid (7.7) is near the low end of the range of n_{Li_2O} slopes (1.6–32.1). Several sets of components have similar slopes (ZrO_2 and SnO_2, SiO_2 and Others, B_2O_3 and Na_2O, and P_2O_5 and CaO). This allows for the possibility of combining components to reduce the number of model terms if desired.

Table V. Summary of Fit and Validation Statistics from Validation Group Fits

Statistics	All Data	Group 1	Group 2	Group 3	Group 4	Group 5	Mean
R^2	0.891	0.894	0.882	0.901	0.891	0.898	0.893
R_A^2	0.885	0.886	0.874	0.893	0.883	0.891	0.885
R_p^2	0.874	0.872	0.859	0.882	0.866	0.877	0.871
R_V^2	—	0.867	0.914	0.839	0.885	0.841	0.869

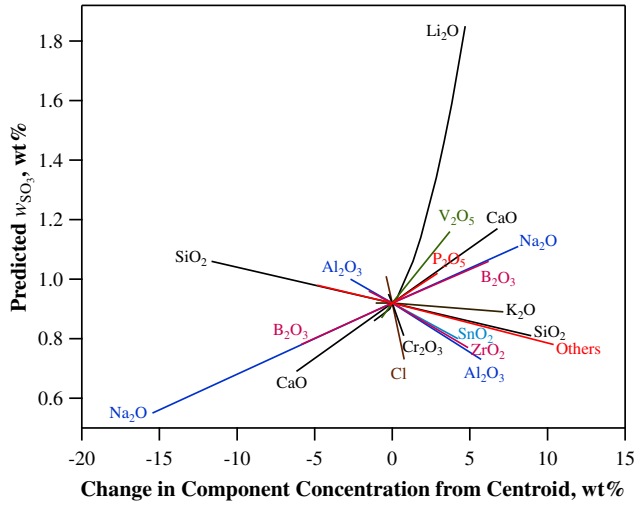

Fig. 5. Effects of component concentration changes on predicted $w_{SO_3}^{Pred}$ at the composition region centroid.

Table VI. Centroid Composition and Component Effect Slopes Calculated at the Centroid

Component	Centroid (wt%)	Slope (wt% SO_3/mass fraction)
Al_2O_3	8.222	−3.314
B_2O_3	9.844	2.322
CaO	6.170	3.721
Cl	0.399	−23.699
Cr_2O_3	0.262	−14.129
K_2O	1.184	−0.337
Li_2O	1.166	7.680
Na_2O	17.932	2.367
P_2O_5	0.155	3.662
SiO_2	41.694	−1.221
SnO_2	0.781	−2.746
V_2O_5	0.687	6.631
ZrO_2	4.136	−2.943
Others	7.369	−1.326

The slope for Li_2O ranges from roughly 1.61 to 32.1 across the model validity range.

The strong positive effects of Li_2O, V_2O_5, and CaO on w_{SO_3} have been reported previously.[3,31,33,41,57] P_2O_5 was reported previously[58] to help increase SO_3 solubility in the melt at lower concentrations and then decrease the solubility at higher concentrations. However, the model suggests a constant improvement for P_2O_5 concentrations up to 3 wt%. Na_2O and B_2O_3 were found to moderately improve solubility (consistent with previous reports[2,4,18,30,31,34–36,38,57]). The very strong tendencies for Cl and Cr_2O_3 to reduce SO_3 solubility are understandable due to their participation in the molten salt. These components have been found to form molten salts even in the absence of SO_3 (see Langowski[59] and references therein for examples). It is anticipated that MoO_3 will likewise promote salt formation, but it was not included as a significant component in the test data used for the work in this paper. ZrO_2 and SnO_2 moderately decrease SO_3 solubility. Finally, it is interesting to note that despite a broad variation in MgO concentrations (up to 10 wt%) and F concentrations (up to 3 wt%), no impacts on SO_3 solubility were evident; hence these components were included in the Others component.

V. Conclusions

An empirical model was developed to predict the solubility of SO_3 in simulated Hanford LAW glasses. This model was found to account for over 87% of the variation in measured solubility (ranging from 0.37 to 2.05 wt% as SO_3 in glass). The model performed equally well when subsets of the data were held out for validation, yielding R_V^2 values roughly the same (0.87) as R^2. The SO_3 solubility model was shown to predict well the maximum amount of SO_3 in melter feed that did not form a salt layer (at least for the 13 compositions under the processing conditions tested) with $R_V^2 = 0.93$ and a RMSPE = 0.086 slightly below the model fit RMSE = 0.12 (which is good). These strong correlations between results from crucible scale solubility testing and melter salt layer formation suggest that, under the conditions used for these tests and the composition region investigated, solubility data from crucible testing can be used to predict SO_3 tolerance in the melter feed. This addresses the long-standing challenge of how to correlate solubility data with the response of dynamic melter process, at least for this limited study. The effects of component concentrations on SO_3 solubility predicted by the empirical model match many of the general trends previously reported in the literature. For example Li_2O, CaO, and V_2O_5 all increase SO_3 tolerance while Cl and Cr_2O_3 decrease it. Some unexpected composition effects were also noticed. For example MgO and F showed little impact.

Acknowledgments

The authors would like to thank the DOE Office of River Protection for their support of this work. The testing results analyzed in this article were generated by the Catholic University of America in support of DOE and were generously shared with the authors for the work in this article. We thank those that participated in the generation of the data, in particular KS Matlack, IL Pegg, and H Gan. DK Peeler and CM Jantzen made valuable contributions to the article through their comments to the initial manuscript. The Pacific Northwest National Laboratory is operated by Battelle for the DOE under contract DE-AC05-76RL01830.

References

[1]J. C. Marra, M. K. Andrews, and R. F. Schumacher, "Vitrification in the Presence of Molten Salts"; pp. 401–8 in *Ceramic Transactions*, Vol. 45, Edited by D. F. Bickford, S. O. Bates, V. Jain, and G. L. Smith. American Ceramic Society, Westerville, OH, 1994.

[2]C. M. Jantzen, M. E. Smith, and D. K. Peeler, "Dependency of Sulfate Solubility on Melt Composition and Melt Polymerization"; pp. 141–52 in *Ceramic Transactions*, Vol. 168, Edited by J. D. Vienna, C. C. Herman, and S. L. Marra. American Ceramic Society, Westerville, OH, 2005.

[3]I. L. Pegg, H. Gan, I. S. Muller, D. A. McKeown, and K. S. Matlack, "Summary of Preliminary Results on Enhanced Sulfate Incorporation During Vitrification of LAW Feeds, VSL-00R3630-1"; ORP-54333. Vitreous State Laboratory, The Catholic University of America, Washington, DC, 2008.

[4]G. K. Sullivan, M. H. Langowski, and P. Hrma, "Sulfate Segregation in Vitrification of Simulated Hanford Nuclear Waste"; pp. 187–93 in *Ceramic Transactions*, Vol. 61, Edited by V. Jain and R. A. Palmer. American Ceramic Society, Westerville, OH, 1996.

[5]D. S. Goldman, "REDOX and Sulfur Solubility in Glass Melts"; pp. 74–91 in *Procedings of the International Congress on Glass*. Charleroi, Belgium, 1985.

[6]H. D. Schreiber, B. K. Kochanowski, C. W. Schreiber, A. B. Morgan, M. T. Coolbaugh, and T. G. Dunlap, "Composition Dependence of REDOX Equilibria in Sodium Silicate Glasses," *J. Non-Cryst. Sol.*, **177**, 340–6 (1994).

[7]H. D. Schreiber, S. J. Kozak, and P. G. Leonhard, "Sulfur Chemistry in A Glass-Forming Borosilicate Melt," *Am. Ceram. Soc. Bull.*, **64** [10] 1339 (1985).

[8]H. D. Schreiber, S. J. Kozak, P. G. Leonhard, and K. K. McManus, "Sulfur Chemistry in a Borosilicate Melt, Part I. REDOX Equilibria and Solubility," *Glastechnische Berichte*, **60** [12] 389–98 (1987).

[9]S. O. Bates, "A Letter Report Summarizing the Sulfate/REDOX Relationship to Glass Melting Chemistry and Behavior, HWVP Baseline Milestone 020207A"; PNNL-23083. Pacific Northwest National Laboratory, Richland, WA, 1985.

[10]J. G. Darab, H. Li, D. W. Matson, P. A. Smith, and R. K. MacCrone, "Chemical and Structural Elucidation of Minor Components in Simulated Hanford Low-Level Waste Glasses"; pp. 237–55 in *Applications of Synchrotron Radiation in Industry, Chemical, and Materials Science*, Edited by L. J. Terminello, K. L. D'Amico, and D. K. Shuh. Plenum, New York, NY, 1996.

[11]H. D. Schreiber, C. W. Schreiber, E. D. Sisk, and S. J. Kozak, "Sulfur Systematics in Model Glass Compositions from West Valley"; pp. 349–58 in *Ceramic Transactions*, Vol. 45, Edited by D. F. Bickford, S. O. Bates, V. Jain, and G. L. Smith. American Ceramic Society, Westerville, OH, 1994.

[12]D. A. McKeown, I. S. Muller, H. Gan, I. L. Pegg, and C. A. Kendziora, "Raman Studies of Sulfur in Borosilicate Waste Glasses"; pp. 451–7 in *Ceramic Transactions*, Vol. 119, Edited by D. R. Spearing, G. L. Smith, and R. L. Putnum. American Ceramic Society, Westerville, OH, 2001.

[13]D. A. McKeown, I. S. Muller, H. Gan, I. L. Pegg, and W. C. Stolte, "Determination of Sulfur Environments in Borosilicate Waste Glasses Using X-ray Absorption Near-Edge Spectroscopy," *J. Non-Cryst. Solids*, **333**, 74–84 (2004).

[14]J. M. Perez, L. J. Ethridge, D. S. Goldman, R. W. Goles, R. D. Peters, N. L. Scharnhorst, and G. J. Sevigny, "West Valley Waste Vitrification Experiment, PSCM-16 Summary"; PNNL-23081. Pacific Northwest National Laboratory, Richland, WA, 1983.

[15]D. A. McKeown, I. S. Muller, H. Gan, I. L. Pegg, and C. A. Kendziora, "Raman Studies of Sulfur in Borosilicate Waste Glasses: Sulfate Environments," *J. Non-Cryst. Solids*, **288**, 191–9 (2001).

[16]R. K. Mishra, K. V. Sudarsan, P. Sengupta, R. K. Vatsa, A. K. Tyagi, C. P. Kaushik, D. Das, and K. Raj, "Role of Sulfate in Structural Modifications of Sodium Barium Borosilicate Glasses Developed for Nuclear Waste Immobilization," *J. Am. Ceram. Soc.*, **91** [12] 3903–7 (2008).

[17]W. Grünewald, G. Roth, S. Hilpp, W. Tobie, A. Salimi, S. Weisenburger, and B. Brendebach, "Laboratory-Scale Development and Technical Demonstration of Borosilicate Glass Tailored for Vitrification of High Sulfur Bearing HLLW"; pp. 392–401 in *Global 2009*, Edited by D. Geneche. Omnipress for the French Nuclear Energy Society, Paris, France, 2009.

[18]M. Lenoir, A. Grandjean, S. Poissonnet, and D. R. Neuville, "Quantitation of Sulfate Solubility in Borosilicate Glasses Using Raman Spectroscopy," *J. Non-Cryst. Solids*, **355**, 1468–73 (2009).

[19]P. A. Bingham, A. J. Connelly, R. J. Hand, N. C. Hyatt, P. A. Northrup, R. A. Mori, P. Glatzel, M. Kavcic, M. Zitnik, K. Bucar, and R. Edge, "A Multi-Spectroscopic Investigation of Sulphur Speciation in Silicate Glasses and Slags," *Glass Technol.-Part A*, **51** [2] 63–80 (2010).

[20]W. K. Kot, H. Gan, and I. L. Pegg, "Sulfur Incorporation in Waste Glass Melts of Various Compositions"; pp. 441–9 in *Ceramics Transactions*, Vol. 107, Edited by G. T. Chandler and X. D. Feng. American Ceramics Society, Westerville, OH, 1999.

[21]D. K. Peeler, C. C. Herman, T. B. Edwards, M. E. Smith, and D. R. Best, "Revisiting the SO_4 Limit for the Defense Waste Processing Facility"; pp. 213–22 in *Ceramic Transactions*, Vol. 176, Edited by C. C. Herman, S. L. Marra, D. R. Spearing, E. R. Vance, and J. D. Vienna. American Ceramic Society, Westerville, OH, 2005.

[22]R. W. Goles, J. A. Del Debbio, R. J. Kirkham, B. D. MacIsaac, J. A. McCray, D. D. Siemer, and N. R. Soelberg, "Test Summary Report INEEL Sodium-Bearing Waste Vitrification Demonstration RSM-01-2"; PNNL-13869. Pacific Northwest National Laboratory, Richland, WA, 2002.

[23]R. W. Goles, J. M. Perez, B. D. MacIsaac, D. D. Siemer, and J. A. McCray, "Test Summary Report INEEL Sodium-Bearing Waste Vitrification Demonstration RSM-01-1"; PNNL-13522. Pacific Northwest National Laboratory, Richland, WA, 2001.

[24]E. Schiewer, H. Rabe, and S. Weisenburger, "The Materials Balance - Scientific Fundamentals for the Quality Assurance of Vitrified Waste"; pp. 289–97 in *Scientific Basis for Nuclear Waste Management V, Materials Research Society Symposium Proceedings*, Vol. 11, Edited by W. Lutze. Elsevier Science Publishing, New York, NY, 1982.

[25]H. L. Hull, "Test Report, Battelle-Pacific Northwest Laboratory: Slurry-Fed Melter Test May 17 - 21, 1982"; DPST-82-718-TL, Savannah River Laboratory, Aiken, SC, 1982.

[26]H. L. Hull, "Test Report, Battelle-Pacific Northwest Laboratory: Slurry-Fed Melter Tests June, August, October 1983"; DPST-84-518, Savannah River Laboratory, Aiken, SC, 1984.

[27]P. Hrma, C. E. Goles, and D. D. Yasuda, "Drainage of Primary Melt in A Glass Batch," *Nucl. Waste Manage. IV*, **23**, 361–7 (1991).

[28]P. A. Smith, J. D. Vienna, and P. Hrma, "The Effects of Melting Reactions on Laboratory-Scale Waste Vitrification," *J. Mater. Res.*, **10** [8] 2137–49 (1995).

[29]P. Hrma, J. D. Vienna, and J. S. Ricklefs, "Mechanism of Sulfate Segregation During Glass Melting"; pp. 147–52 in *Scientific Basis for Nuclear Waste Management XXVI, Materials Research Society Symposium Proceedings* Vol. 757, Edited by R. J. Finch and D. B. Bullen. Materials Research Society, Warrendale, PA, 2003.

[30]J. G. Darab, D. D. Graham, B. D. MacIssac, R. L. Russell, H. D. Smith, J. D. Vienna, and D. K. Peeler, "Sulfur Partitioning During Vitrification of INEEL Sodium Bearing Waste: Status Report"; PNNL-13588. Pacific Northwest National Laboratory, Richland, WA, 2001.

[31]J. D. Vienna, W. C. Buchmiller, J. V. Crum, D. D. Graham, D.-S. Kim, B. D. Macisaac, M. J. Schweiger, D. K. Peeler, T. B. Edwards, I. A. Reamer, and R. J. Workman, "Glass Formulation Development for INEEL Sodium-Bearing Waste"; PNNL-14050. Pacific Northwest National Laboratory, Richland, WA, 2002.

[32]D. D. Walker, "Sulfate Solubility in DWPF Glass"; DPST-82-622, Savannah River Laboratory, Aiken, SC, 1982.

[33]J. D. Vienna, P. Hrma, W. C. Buchmiller, and J. S. Ricklefs, "Preliminary Investigation of Sulfur Loading in Hanford LAW Glass"; PNNL-14649. Pacific Northwest National Laboratory, Richland, WA, 2004.

[34]K. Papadopoulos, "The Solubility of SO_3 in Soda-Lime-Silica Melts," *Phys. Chem. Glasses*, **14** [3] 60–5 (1973).

[35]H. Li, P. Hrma, and J. D. Vienna, "Sulfate Retention and Segregation in Simulated Radioactive Waste Borosilicate Glass"; pp. 237–46 in *Ceramic Transactions*, Vol. 119. Edited by D. R. Spearing, G. L. Smith, and R. L. Putnum. American Ceramic Society, Westerville, OH, 2001.

[36]M. Ooura and T. Hanada, "Compositional Dependance of Solubility of Sulphate in Silicate Glasses," *Glass Technol.*, **39** [2] 68–73 (1998).

[37]A. D. Pelton, "Thermodynamic Calculations of Chemical Solubilities of Gases in Oxide Melts and Glasses," *Glastechnische Berichte*, **72** [7] 214–26 (1999).

[38]H. D. Schreiber and M. E. Stokes, "Enhancing the Sulfate Capacity of Glasses for Nuclear Waste Immobilization," *J. Undergraduate Chem. Res.*, **2**, 53–8 (2002).

[39]D. K. Peeler, C. C. Herman, M. E. Smith, T. H. Lorier, D. R. Best, T. B. Edwards, and M. A. Baich, "An Assessment of the Sulfate Solubility Limit for the Frit 418 – Sludge Batch 2/3 System"; WSRC-TR-2004-00081. Westinghouse Savannah River Company, Aiken, SC, 2004.

[40]T. H. Lorier, I. A. Reamer, and R. J. Workman, "Initial Sulfate Solubility Study for Sludge Batch 4 (SB4)"; WSRC-TR-2005-00213. Westinghouse Savannah River Company, Aiken, SC, 2005.

[41]D. Manara, A. Grandjean, O. Pinet, J. L. Dussossoy, and D. R. Neuville, "Sulfur Behavior in Silicate Glasses and Melts: Implications for Sulfate Incorporation in Nuclear Waste Glasses as a Function of Alkali Cation and V_2O_5 Content," *J. Non-Cryst. Solids*, **353**, 12–23 (2007).

[42]P. A. Bingham and R. J. Hand, "Sulphate Incorporation and Glass Formation in Phosphate Systems for Nuclear and Toxic Waste Immobilization," *Mater. Res. Bull.*, **43** [7] 1679–93 (2008).

[43]P. A. Bingham, A. J. Connelly, R. J. Hand, N. C. Hyatt, and P. A. Northrup, "Incorporation and Speciation of Sulphur in Glasses for Waste Immobilisation," *Glass Technol.: Eur. J. Glass Sc. Technol. A*, **50** [3] 135–8 (2009).

[44]A. L. Billings and K. M. Fox, "Retention of Sulfate in Savannah River Site High-Level Radioactive Waste Glass," *Int. J. Appl. Glass Sci.*, **1** [4] 388–400 (2010).

[45]I. S. Muller, I. L. Pegg, A. C. Buechele, H. Gan, C. Kim, S. T. Lai, G. del Rosario, and Q. Yan, "Glass Formulation and Testing with TWRS LAW Simulants"; ORP-56328. Vitreous State Laboratory, The Catholic University of America, Washington, DC, 1998.

[46]I. S. Muller, A. C. Buechele, and I. L. Pegg, "Glass Formulation and Testing with RPP-WTP LAW Simulants, VSL-01R3560-2"; ORP-56327. Vitreous State Laboratory, The Catholic University of America, Washington, DC, 2001.

[47]I. S. Muller and I. L. Pegg, "Baseline LAW Glass Formulation Testing, VSL-03R3460-1"; ORP-55237. Vitreous State Laboratory, The Catholic University of America, Washington, DC, 2003.

[48]K. S. Matlack, M. Chaudhuri, H. Gan, I. S. Muller, W. K. Kot, W. Gong, and I. L. Pegg, "Glass Formulation Testing to Increase Sulfate Incorporation, VSL-04R4960-1"; ORP-51808. Vitreous State Laboratory, The Catholic University of America, Washington, DC, 2005.

[49]K. S. Matlack, W. Gong, I. S. Muller, I. Joseph, and I. L. Pegg, "LAW Envelope C Glass Formulation Testing to Increase Waste Loading, VSL-05R5900-1"; ORP-56323. Vitreous State Laboratory, The Catholic University of America, Washington, DC, 2006.

[50]K. S. Matlack, W. Gong, I. S. Muller, I. Joseph, and I. L. Pegg, "LAW Envelope A and B Glass Formulations Testing to Increase Waste Loading, VSL-06R6900-1"; ORP-56322. Vitreous State Laboratory, The Catholic University of America, Washington, DC, 2006.

[51]K. S. Matlack, I. Joseph, W. Gong, I. S. Muller, and I. L. Pegg, "Enhanced LAW Glass Formulation Testing, VSL-07R1130-1"; ORP-56293. Vitreous State Laboratory, The Catholic University of America, Washington, DC, 2007.

[52]K. S. Matlack, I. Joseph, W. Gong, I. S. Muller, and I. L. Pegg, "Glass Formulation Development and DM10 Melter Testing with ORP LAW Glasses, VSL-09R1510-2"; ORP-56296. Vitreous State Laboratory, The Catholic University of America, Washington, DC, 2009.

[53]I. S. Muller, K. S. Matlack, H. Gan, I. Joseph, and I. L. Pegg, "Waste Loading Enhancements for Hanford LAW Glasses, VSL-10R1790-1"; ORP-48578. Vitreous State Laboratory, The Catholic University of America, Washington, DC, 2010.

[54]G. F. Piepel, J. M. Szychowski, and J. L. Loeppky, "Augmenting Scheffe Linear Mixture Models with Squared and/or Crossproduct Terms," *J. Qual. Technol.*, **34** [3] 297–314 (2002).

[55]G. F. Piepel, "A Component Slope Linear Mixture Model for Mixture Experiments," *Qual. Technol. Quantitative Manage.*, **4** [3] 331–43 (2007).

[56]J. A. Cornell, *Experiments with Mixtures*, 3rd edition. John Wiley and Sons, New York, NY, 2002.

[57]M. J. Plodinec and J. R. Wiley, "Evaluation of Glass as a Matrix for Solidifying Savannah River Plant Waste: Properties of Glasses Containing Li_2O"; DP-1498, Savannah River Laboratory, Aiken, SC, 1979.

[58]H. Li, J. G. Darab, D. W. Matson, P. A. Smith, P. Hrma, Y. Chen, and J. Liu, "Phosphate-Sulfate Interaction in Simulated Low-Level Radioactive Waste Glasses"; pp. 141–8 in *Scientific Basis for Nuclear Waste Management XIX, Materials Research Society Symposium Proceedings*, Vol. 412, Edited by W. M. Murphy and D. A. Knecht. Materials Research Society, Pittsburgh, PA, 1996.

[59]M. H. Langowski, "The Incorporation of P, S, Cr, F, Cl, I, Mn, Ti, U, and Bi into Simulated Nuclear Waste Glasses: Literature Study"; PNNL-10980, Pacific Northwest National Laboratory, Richland, WA, 1996. □